Single-cell analysis of the Dps response to oxidative stress

De Martino, Michela; Ershov, D.; van den Berg, P.J.; Tans, Sander J.; Meyer, Anne S.

DOI
10.1128/JB.00239-16

Publication date
2016

Document Version
Accepted author manuscript

Published in
Journal of Bacteriology

Single-cell analysis of the Dps response to oxidative stress

Authors

Michela De Martino[a], Dmitry Ershov[b], Peter J. van den Berg[a], Sander J. Tans[b], Anne S. Meyer[a,#]

Department of Bionanoscience, Kavli Institute of Nanoscience, Delft University of Technology, Delft, The Netherlands[a] ; FOM institute AMOLF, Amsterdam, The Netherlands[b].

Address correspondence to Anne S. Meyer, e-mail: a.s.meyer@tudelft.nl, phone: +31-(0)152789249, fax: +31-(0)152781202

Running title: Single-cell analysis of Dps response

Abstract

Microorganisms have developed an elaborate spectrum of mechanisms to respond and adapt to environmental stress conditions. Among these is the expression of *dps*, coding for the DNA-binding protein from starved cells. Dps becomes the dominant nucleoid-organizing protein in stationary-phase *Escherichia coli* cells and is required for robust survival under stress conditions including carbon or nitrogen starvation, oxidative stress, metal exposure, and irradiation. To study the complex regulation of Dps in *E. coli*, we utilized time-lapse fluorescence microscopy imaging to examine the kinetics, input-encoding, and variability of the Dps response in single cells. In the presence of an oxidative stressor, we observed a single pulse of activation of Dps production. Increased concentrations of H_2O_2 led to increased intensity and duration of the pulse. While lower concentrations of H_2O_2 robustly activated the Dps response with little effect on growth rate, higher concentrations of H_2O_2 resulted in dramatically slower and highly variable growth rates. Comparison of cells within the same concentration of H_2O_2 revealed that increased levels of Dps expression did not confer a growth advantage, indicating that recovery from stress may rely primarily upon variation in the amount of damage caused to individual cells.

Importance

We show for the first time the response of the DNA-binding protein from starved cells (Dps) to oxidative stress in single cells of *E. coli*. Through time-lapse fluorescence microscopy, a single pulse of Dps production is observed in cells exposed to H_2O_2, with a duration and intensity of the induction proportional to the concentration of the applied stress. A more intense Dps expression did not provide a growth benefit to the bacteria, suggesting that

healing from oxidative stress may largely depend upon the amount of damage in each individual cell.

Introduction

Bacteria encounter many stresses during their development, and they need to be able to adapt quickly to the environment to survive. Bacterial response mechanisms frequently involve specific sets of genes activated to help the cell adapt to the stress. Alternative sigma factors, of which *Escherichia coli* has seven, are a frequent regulatory mechanism (1). While housekeeping genes expressed during exponential growth are controlled by the transcription factor σ^{70} (2, 3), alternative sigma factors act as transcription initiation factors to control the activation of specialized regulons during specific growth or stress conditions (4). The general stress response sigma factor σ^{S} activates the transcription of more than 70 genes, conferring resistance to carbon/phosphate/nitrogen starvation, heat shock, high/low pH, UV-radiation, and oxidative stress, among others (5, 6).

Microorganisms living in an aerobic environment unavoidably encounter oxidative stress as a by-product of their aerobic metabolism (7). The resultant formation of reactive oxygen species (ROS) can lead to the damage of cellular components including membranes, DNA, and proteins (8). As an adaptation to this condition, bacteria produce enzymes such as superoxide dismutases and reductases to scavenge these toxic components (9). Additionally, cells also face external sources of oxidative stress: macrophages produce superoxide and nitric oxide to kill invading bacteria (10); following perception of pathogens, plants also induce the synthesis of organic peroxides (11); certain communities of microorganisms

57 excrete ROS to inhibit the growth of their competitors (12); and exposure to environmental
58 redox cycling compounds can cause damaging intracellular redox reactions (13).

59 In this challenging environment, bacteria have developed refined molecular mechanisms of
60 defense. The DNA-binding protein from starved cells (Dps) plays a crucial role during stress
61 exposure. *Escherichia coli dps* mutants experience a severe reduction in survival when
62 exposed to any of several different stressors including oxidative stress, heat shock, metal
63 exposure, UV and gamma irradiation, or extreme pH (14-16). Additionally, Dps was shown to
64 protect cells against DNA strand breakage (17). In *E.coli*, the protective effect of Dps is
65 attributed to its dual biochemical functions. Dps has the ability to bind DNA and form Dps-
66 DNA crystals, which may provide mechanical shielding against damaging agents (14, 18, 19).
67 The ferroxidase activity of Dps may also contribute significantly to its protective abilities.
68 Hydroxyl radicals can be formed intracellularly through chemical reaction between ferrous
69 iron and H_2O_2, either internally generated or derived from the environment. Dps catalyzes
70 the oxidation of ferrous iron, preferring H_2O_2 as a reactant rather than O_2, thereby
71 preventing the formation of hydroxyl radicals (20). Dps oligomers are composed of 12
72 identical monomers, each one folded into a compact four-helix bundle (21), surrounding a
73 central cavity that can store up to 500 iron atoms (22). The DNA-binding and ferroxidase
74 activities of Dps are biochemically separable, but they both contribute to maintain DNA
75 integrity and cellular viability (23).

76 Intracellular Dps levels are controlled by a complex regulatory network. During the transition
77 from exponential to stationary phase, the number of Dps molecules within a single *E. coli*
78 bacterium increases from approximately 6000 to 180,000, whereby it becomes the most
79 abundant DNA-binding protein (24). *dps* is transcribed from a single promoter recognized by

either the σ^{70} (housekeeping) or σ^{S} (stationary phase) sigma factor in response to different growth and environmental conditions (25-27). In exponential growth, *dps* can be activated in an OxyR-dependent manner by treatment of the cells with H_2O_2, recruiting σ^{70} to initiate transcription. During stationary phase or carbon starvation, σ^{S} controls *dps* expression (25). When bacteria are growing exponentially and not exposed to stress, the *dps* promoter is downregulated by two nucleoid-binding proteins: Fis and H-NS (26, 28).

Despite the knowledge acquired in recent years, the behavior of the Dps response is not understood at the single-cell level. Upon exposure to oxidative stress, each cell that sustains oxidative damage will require sufficient upregulation of enzymes that can counteract the damage in order to maintain its health. However, the high-resolution fluctuations of Dps production levels over time and the intensity and duration of Dps production during the Dps response are still unknown at the single-cell level as well as in bulk cultures. Very little is known also about the variability of the Dps stress response in individual cells and its effect on cellular growth rate, which could play a crucial role in the ability of a bacterial population to maintain competitive advantage in adverse environmental conditions. In addition, it is unknown how the dynamics of Dps production are affected when the concentration of stressor is varied, a question that is central to the ability of a cell to respond appropriately to changes in its environment. Clear insights into these biological processes require recently developed single-cell technologies to overcome the limitations of bulk experiments, allowing for quantification of the cell-to-cell variability in a population as well as characterization of the dynamics of stress responses (29-35).

In this work, we examined the kinetics and variability of activation of Dps production at the single-cell level upon exposure to different levels of oxidative stress. We observed one single

pulse of Dps production, with an intensity and duration proportional to the concentration of H_2O_2 applied, until the highest concentration of H_2O_2 resulted in saturation of the intensity but not the duration of Dps production. Cell growth was not linearly correlated with the H_2O_2 concentration, such that low concentrations resulted in robust Dps production but only a minor decrease in initial growth rate. Higher concentrations of H_2O_2 were associated with major reductions in growth rate, accompanied by dramatically increased variation. A comparison of bacteria that were exposed to the same concentration of stressor revealed that higher levels of Dps production were associated with similar or slower growth compared to cells with lower Dps production. This behavior was perhaps due to variation in the amount of damage experienced by individual cells that drove both reduced growth and increased Dps production.

Materials and Methods

dps-mCherry strain construction

The *E. coli dps-mCherry* strain was created from the *E. coli* K-12 strain W3110 (CGSC# 4474) by replacement of the genomic *dps* gene by a counter-selectable *cat-sacB* cassette (23) and subsequent replacement with a *dps-mCherry* cassette.

The *dps-mCherry* cassette was created using an adapted version of the Gibson DNA assembly protocol (36) and introduced into the pBAD33 plasmid to create the pM1 plasmid. The backbone plasmid pBAD33 (37) was amplified using PCR to create compatible ends for recombination with the *dps-mCherry* cassette. The following primers were used: forward MDM1 5'-GATCCCCGGGTACCGAGCTC-3' and reverse MDM2 5'-CAAGCTTGGCTGTTTTGGCG-3'. The *mCherry* gene was amplified using PCR from the plasmid pROD22 (38) to introduce

the *dps* ribosome binding site (RBS) sequence immediately upstream of the *mCherry* gene. The following primers were used (the sequence of the RBS is underlined): forward MDM3 5'-CATCAAGAGGATATGAAATTATGGCTATCATTAAAGAGTTC-3' and reverse MDM4 5'-TTACTTGTACAGCTCGTCCATGC-3'. This RBS-*mCherry* PCR product was further amplified to introduce an upstream flanking sequence homologous to the *dps* gene and a 30-bp downstream flanking sequence homologous to the pBAD33 plasmid. The following primers were used (the sequences of the homologous regions are underlined): forward MDM5 5'-GTTTATCGAGTCTAACATCGAATAACATCAAGAGGATATGAAATTATG-3' and reverse MDM6 5'-TTCTCTCATCCGCCAAAACAGCCAAGCTTGTTACTTGTACAGCTCGTCC-3'. The *dps* gene was amplified from the pET17b-dps plasmid (23) to introduce a 30-bp upstream flanking sequence homologous to the plasmid pBAD33 and a downstream flanking sequence homologous to the RBS-*mCherry* gene. The following primers were used (the sequences of the homologous regions are underlined): forward MDM7 5'-TAGCGAATTCGAGCTCGGTACCCGGGGATCATGAGTACCGCTAAATTAGT-3' and reverse MDM8 5'-CATAATTTCATATCCTCTTGATGTTATTCGATGTTAGACTCGATAAAC-3'.

The three fragments were DpnI (New England Biolabs (NEB))-digested at 37°C for 1 hour and purified with Wizard® SV Gel and PCR Clean-Up System (Promega), then assembled using Gibson DNA assembly (36). The assembly reaction was prepared by combining 15 µL of Gibson assembly master mix (320 µL of 5X ISO buffer [0.5 M Tris-HCl (Sigma) pH 7.5, 50 mM $MgCl_2$, 4 mM dNTP (Invitrogen) mix (equal concentration of the four nucleotides), 50 mM DTT (Sigma), 25% w/v PEG-8000 (Sigma), 5 mM NAD (NEB)], 0.64 µL of 10 U μL^{-1} T5 exonuclease (Epicentre), 20 µL of 2 U μL^{-1} Phusion polymerase (Finnzymes), 160 µL of 40 U μL^{-1} Taq ligase (NEB), dH_2O to 1.2 ml), 100 ng of linearized vector backbone, and 100 ng of each assembly fragment in a total volume of 20 µL. The reaction was incubated at 50°C for

60 min. Electrocompetent *E. coli* W3110 cells were transformed with 5 µL of the assembly reaction using electroporation. The positive colonies carrying the chloramphenicol resistance gene from the pBAD33 plasmid were identified, and the accuracy of the sequence was checked with sequencing analysis.

The *dps-mCherry* cassette was amplified from the pM1 plasmid using PCR to introduce 50-bp flanks homologous to the chromosomal *dps* flanks. The following primers were used (the sequences of the homologous regions are underlined): forward MDM9 5'-TACTTAATCTCGTTAATTACTGGGACATAACATCAAGAGGATATGAAATTATGAGTACCGCTAAATTAG-3' and reverse MDM10 5'-AGGAAGCCGCTTTTATCGGGTACTAAAGTTCTGCACCATCAGCGATGGATTTACTTGTACAGCTCGTCCA-3'. The fragment was DpnI-digested and purified, then introduced with electroporation into a W3110 *dps::cat-sacB* strain (23). Homologous recombination was allowed to occur for 3 hours in LB medium at 37°C while shaking at 250 rpm, and cells were plated on NaCl-free LB 10% sucrose agar (counterselective for *sacB*). Plates were incubated overnight at 30°C. Healthy-looking colonies were re-streaked on LB agar containing 25 µg mL^{-1} chloramphenicol. Colonies that did not grow on chloramphenicol were screened using colony PCR, and gene replacement was verified by sequence analysis. The *mCherry* expression was confirmed with fluorescence-activated cell sorting (FACS) (data not shown).

Growth conditions for microscopy

For the single-cell microscopy experiments, one colony of *dps-mCherry* was inoculated overnight into Hi-Def Azure medium (3H500, Teknova) supplemented with 0.2% glucose and grown overnight at 37°C. This preculture was diluted 1:100 and grown for around 2 hours at

37°C until early exponential phase ($O.D._{600}$ 0.2-0.3). The culture was diluted to $O.D._{600}$=0.005 for seeding onto the agarose pad.

Agarose pad preparation

Agarose pads were prepared with a modified version of the protocol in (39). The pads were prepared freshly for each experiment. 2% (w/v) low-melt Agarose LE (V3125, Promega) was added to 5 mL of Hi-Def Azure medium and dissolved by microwaving. After the agarose solution had cooled, H_2O_2 was added. Agarose pads were formed immediately thereafter. Cover glass slides of 20 mm^2 (631-0122, VWR) were placed on Parafilm M® (Bemis Company, Inc.), and 900 µL of agarose were pipetted onto each. Immediately after pipetting, a second cover glass was placed on top of the agarose. The pads were allowed to solidify for 45–60 min at room temperature while covered with a lid to prevent edge evaporation. When the agarose was solidified, it was cut into pads of 0.5 x 0.5 cm. 2 µL of bacterial culture diluted to $O.D._{600}$ 0.005 was seeded onto individual agarose pads. The culture was allowed to evaporate and absorb into the agarose for about 10 min at room temperature. When the surface appeared to be dry, the pad was flipped with a scalpel onto a 4-well slide-base tissue culture chamber (Starstedt). The chamber was closed with a lid and sealed with Parafilm M® to avoid evaporation during the imaging. The cells were able to grow in a monolayer due to their placement between the glass bottom of the chamber and the agarose pad on top.

The variability of H_2O_2 distribution in the pads was determined using rhodamine as a fluorescent reporter. During the preparation of the agarose pads, dihydrorhodamine 123 (D1054, Sigma-Aldrich) was added to a final concentration of 20 µM after the agarose solution had cooled, and the pads were formed immediately thereafter. The pads were

scanned using a Typhoon Trio (Amersham Biosciences), and the images were analyzed using ImageJ software (40). The fluorescence intensity values of 80 different pixels in 2 different pads were averaged, and the standard deviation was calculated, showing an upper limit of variability of 12.9%. We expect a lower variability for the H_2O_2 molecule than for rhodamine, since the diffusion coefficient of H_2O_2 is 1 order of magnitude larger than that of rhodamine: $1.305\pm0.83\times10^{-5}$ cm^2s^{-1} (41) and $4x10^{-6}$ cm^2 s^{-1} respectively (42).

Fluorescence microscopy

Microcolonies on agarose pads were imaged by time-lapse fluorescence microscopy using an inverted microscope (Olympus IX81), an AMH-200 lamp (Andor), and a Cy3 filter cube (4040C). Images were acquired with Luca R EMCCD camera (Andor). Andor iQ software was used to control the microscope and to perform automatic imaging acquisition. Experiments were performed at 37°C using an incubation chamber (H201-T, Okolab) to allow precise temperature control. Phase contrast images (500 ms exposure time, 3 images +/- 0.2 µm from the focus) and fluorescence images (100 ms exposure time) were recorded every 5 min, for 3-4 hours.

Data analysis

Images were analyzed using a custom Matlab program (43) based on the Schnitzcells program (39). Data analysis consisted of three steps: segmentation, tracking, and extraction of cell parameters. Each phase contrast image (average of three) was segmented: the background was separated from the cells, and clumps of cells were cut based on concavity and phase contrast maxima. Then the outline of each individual cell was detected. Cell

edges were determined using Laplacian of Gaussian filter. The segmentation of the cells was checked and corrected manually when necessary. Next, tracking was performed, in which cell lineages were traced by a tracking algorithm that searches for nearby cells in successive frames. Lastly, cell length was extracted from segment properties, and growth rate was determined from exponential fits of lengths-in-time. Individual cell fluorescence was extracted from fluorescent images using segmentation obtained from phase contrast images (for more details on analysis see Supplemental material). For each microcolony, the fluorescence intensity curves were fitted with the best-fitting polynomial (degree 5), and the maximum of this function was considered to be the maximum fluorescence intensity. Dps production activity is defined as the rate of mCherry protein production (33, 35, 39, 44). The duration of Dps production was calculated as time from the beginning of the exposure to H_2O_2. Between 11 and 19 colonies for each stress condition were analyzed for a total of 75 colonies.

Results

Construction of a reporter strain for Dps production

To explore Dps production dynamics, we constructed a reporter strain of *E. coli* (named "*dps-mCherry*"), with the *mCherry* gene introduced as a reporter for Dps production. The two genes are both present in the *dps* promoter, with *mCherry* immediately downstream of *dps*. A ribosome binding site (RBS) sequence identical to that of the *dps* RBS was placed upstream of the *mCherry* reporter gene (Fig. S1). This construct allowed the detection and the quantification of Dps production activity in single cells through monitoring of the collective fluorescence emitted by the fluorescent proteins. In order to characterize the

health of the *dps-mCherry* strain, we compared its growth with the wild-type parental strain in the presence of H_2O_2 concentrations between 0 and 10 mM. Both the strains showed a similar growth response (Fig. S2). The growth kinetics were comparable at concentrations of H_2O_2 up to 1 mM, showing similar robust exponential-phase kinetics and final optical densities. At higher concentrations of H_2O_2, both strains showed growth inhibition. Thus, the engineered *dps-mCherry* strain exhibits similar growth response to H_2O_2 as the wild-type strain.

To verify Dps production, both strains were exposed to 0, 0.5, and 1 mM H_2O_2, and Dps protein levels were analyzed through Western blotting. An increase in Dps concentration, proportional to the stressor concentration, was detected in both strains in the presence of H_2O_2 (Fig. S3).

An engineered strain carrying a chimeric version of *dps*, fused C-terminally to the *mCherry* gene as translational reporter, was also constructed. Cells expressing this protein showed a non-homogeneous distribution of fluorescence throughout the cell volume, with visible puncta of more intense fluorescence (data not shown). Previous work has similarly shown that fusion of Dps with the GFP protein resulted in aggregation of this fusion protein in *E. coli* cells (45). This strain was therefore excluded from further experimentation.

Dps production dynamics during oxidative stress

Cells exposed to concentrations of H_2O_2 between 0 and 100 µM were analyzed using quantitative time-lapse fluorescence microscopy to detect Dps protein production, defined as the rate of mCherry protein production (33, 35, 39, 44), in each individual cell over time. The *E. coli* cells were grown in rich defined medium to early exponential phase, then

transferred to an agarose pad in which H_2O_2 was incorporated, to begin the application of oxidative stressors. Individual cells grew and divided over time to give rise to a microcolony. A difference in growth and fluorescence could be observed in cells not exposed to any stressor compared to those in the presence of different concentrations of H_2O_2. In the colonies without applied stress, we observed that the fluorescence of each cell is indistinguishable from background during the entire duration of the measurement (Fig. S4 A). In the presence of H_2O_2, we detected a fluorescent signal that was roughly proportional to the amount of applied stress (Fig. S4 B-E). We observed a general trend for the intensity of the fluorescence signal over time: the intensity increased during the initial period of the measurement and then decreased thereafter. Reduced growth was apparent at higher concentrations of H_2O_2, and at 100 µM H_2O_2 there was a near-complete inhibition of cell division (Fig. S4 D-E).

The data was analyzed using modified Schnitzcells software (39) to extract the fluorescence intensity within single cells as mean fluorescence per unit area (43). In the absence of oxidative stress, the fluorescence intensity of each individual cell present within a microcolony over time was very low (Fig. 1 A). Exposure to hydrogen peroxide induced a single pulse of fluorescence that started shortly after the cell progenitor of the colony first experienced the stress, in every individual cell analyzed (100%) (Fig. 1 B-E). The pulse was highly synchronized between the individual cells within each microcolony population throughout the duration of the imaging. The variability of fluorescence signal among cells within a colony at each time point was evaluated by calculation of the coefficient of variation (CV) as the ratio of the standard deviation to the mean. As the single cells divided to form a small microcolony over the course of the experiment, the CV remained low, between 0.0 and 0.25, for colonies exposed to 0, 50, or 100 µM H_2O_2. For cells exposed to 10 or 30 µM

290 H_2O_2, the CV increased steadily over time to reach values around 0.5 (Fig. 1 F). This increase
291 in CV over time might be due to an asymmetric division of oxidative components or mCherry
292 molecules among individual bacteria as the cell population increases through cell division.
293
294 In order to compare fluorescent responses between microcolonies, we calculated the
295 average of the fluorescence values of all cells within a microcolony, at each time point
296 measured (Fig. 2). Every colony grown in the absence of stressor showed a low average
297 fluorescence signal that decreased slightly over the duration of the imaging (Fig. 2 A). The
298 colonies exposed to 10, 30, or 50 µM H_2O_2 showed a similar fluorescence profile: a large
299 transient increase in fluorescence over time that took the form of one major peak. Colonies
300 exposed to the same amount of hydrogen peroxide showed varying peak amplitudes and
301 durations (Fig. 2 B-D). In contrast, at 100 µM H_2O_2 no peak of fluorescence was detected.
302 Instead, the average fluorescence signal in each colony rose to a plateau, over a variable
303 period of time (Fig. 2 E). Calculation of the average fluorescence profile over time for all
304 colonies within each experimental condition revealed that increasing concentrations of H_2O_2
305 resulted in both an increase of the intensity and the duration of fluorescence signal. The
306 standard deviations associated with certain conditions showed a large overlap, especially
307 between 50 µM and 100 µM (Fig. 2 F). The variability of the average fluorescence signal
308 among different microcolonies in the same stress condition was evaluated by calculation of
309 the coefficient of variation at each time point. The CV values observed at 0, 30, and 100 µM
310 H_2O_2 remained around 0.3, while at 10 and 50 µM H_2O_2 the CV values were higher, reaching
311 a maximum value of around 0.6 at 10 µM and 0.9 at 50 µM H_2O_2 before decreasing again
312 (Fig. 2 G).
313

To assess whether the observed dynamics of Dps induction were an artifact of the experimental procedure, several control experiments were performed. To determine the consequences of the light exposure on the mCherry protein during the time-lapse fluorescence microscopy process, a photobleaching test was performed on a strain of *E. coli* with constitutive *mCherry* expression (Supporting information). We observed an average of about 20% decrease in the fluorescence signal due to the cumulative photobleaching effect of our image acquisition process on a single cell (Fig. S5). To test the effect of imaging on the cellular fluorescence, images of the *dps-mCherry* strain in the presence of 30, 50, or 100 µM H_2O_2 were acquired every 30 minutes. These fluorescence curves showed a shape similar to those obtained from image acquisition every 5 minutes (Fig. S6, Fig. 2) demonstrating that that the imaging process does not significantly affect the measured cellular behavior. Similarly shaped peaks of fluorescence were observed both in the agarose pad system and in a microfluidics device (46) in which H_2O_2 was constantly applied to the cells over the duration of the imaging (Fig. S7), indicating that the shape of the fluorescence curve is not due to degradation of H_2O_2 over time. The stability of mCherry signal in the presence of the oxidating effect of 50 and 100 µM H_2O_2 was also investigated, showing no statistically significant difference in mCherry degradation or loss of fluorescence intensity due to oxidation (Fig. S8).

Correlations between oxidative stressor concentration and the intensity and duration of Dps production

For a quantitative analysis of Dps induction in the presence of oxidative stress, we analyzed the intensity and the length of the fluorescence peak. For each microcolony, the curve representing the average fluorescence intensity among its constituent cells was fitted with a

polynomial function in order to extract both the maximum value of the fluorescence and the time point at which it was reached. These values were calculated from averaged microcolony fluorescence values since individual cells within each microcolony showed low variability in fluorescence at timepoints before the peak of fluorescence was reached (Fig. 1F). Calculation of the average maximum fluorescence values of colonies exposed to the same amount of H_2O_2 revealed that higher concentrations of stressor were correlated with higher peak amplitude for H_2O_2 concentrations between 0 µM and 50 µM (Fig. 3 A). No increase in average maximum fluorescence value was observed when the H_2O_2 concentration was increased from 50 µM to 100 µM (Fig. 3 A). The variability in the maximum fluorescence intensity among different colonies in the presence of the same concentration of stressor was evaluated by calculation of the coefficient of variation. These values ranged between 0.23 and 0.47, with the maximum variability observed at 10 µM H_2O_2 (Fig. 3 B). No overall trend was seen between the coefficient of variation and the maximum fluorescence values over the various concentrations of H_2O_2 (Fig. 3 C). No significant differences were observed in the distribution of maximum fluorescence values when microcolonies were grown on the same agarose pad versus different agarose pads.

The average time at which the maximum fluorescence signal was observed for microcolonies in each experimental condition increased steadily with the amount of H_2O_2 applied to the culture (Fig. 4 A). The coefficient of variation for the time of maximum fluorescence intensity was calculated between different microcolonies in the same stress condition and ranged between 0.10 and 0.29, lower than the variability observed for the strength of the induction (Fig. 4 B). No relationship was observed between the coefficient of variation values and the time to the maximum fluorescence, over the concentrations of H_2O_2 (Fig. 4 C). Taken together, our data indicate that an increase in hydrogen peroxide concentration led to an

362 increase of Dps production activity. In addition, the duration of the protein synthesis also
363 increased with the concentration of the stressor.

364 Correlation analyses were performed on the extracted values for the maximum fluorescence
365 intensity and the duration of the increase in fluorescence for individual microcolonies. When
366 comparing all the stress conditions simultaneously, the Pearson correlation coefficient (R)
367 between the time to reach the fluorescence peak and its intensity was 0.80 with a p value <
368 0.0001 (Fig. 5 A). Fluorescence peaks that were higher in amplitude were therefore strongly
369 correlated with a longer period of Dps production. While this strongly positive correlation
370 was observed through analyzing the pooled data, the data for each individual H_2O_2
371 concentration considered separately showed a weaker positive correlation, ranging from
372 0.23 to 0.82 with an average of 0.49 (Fig. 5 A).

373 ## Effects of oxidative stress on cellular growth
374

375 To analyze the effect of oxidative stress on cellular morphology, the parameter of cell length
376 was calculated as the length of the axis between the two poles of a cell (43). We compared
377 the average length of all cells within each microcolony over time for all the microcolonies
378 analyzed (Fig. S9). If 0 µM or 10 µM H_2O_2 was applied, we observed the trend that the cell
379 length slightly decreased over time, declining from an average of 5.5 µm down to 3.5 µm
380 (Fig. 6, Fig. S9 A-B). Application of higher H_2O_2 concentrations of 30 µM or 50 µM resulted in
381 little increase in the average cell length, but a higher proportion of elongated cells, reaching
382 a length of up to 12.5 µm (Fig. 6, Fig. S9 C-D). The highest concentration of H_2O_2 applied, 100
383 µM, caused a complete halt of cell growth and division; each cell remained at the same
384 length throughout the course of the experiment. (Fig. 6, Fig. S9 E). The standard deviation

for average cell length per microcolony overlapped greatly between conditions, such that the amount of stressor applied is a poor predictor of cell length (Fig. 6). We observed that the variability of cell length increased over time for colonies exposed to 0-50 µM H_2O_2, rising from near-zero at the start of imaging to 0.6, but remained close to zero for 100 µM H_2O_2 (Fig S9 F).

We also evaluated cellular growth rate over time upon exposure to oxidative stress. The instantaneous growth rate, µ, was calculated by fitting the cell length over time to an exponential function (43). Cell width was not seen to vary significantly during the experiments. We calculated the average instantaneous growth rate of all the cells within a microcolony at each point in time (Fig. 7). The cells exposed to either 0 µM or 10 µM hydrogen peroxide showed a similar, slightly increasing growth rate over time, ranging between 1.1 and 1.8 µ h^{-1} (Fig. 7 A-B). Each further increase of the stressor concentration led to a reduction of cell growth. We observed that at 30 µM H_2O_2 the colonies grew only moderately during the initial part of the experiment, with an average starting growth rate of approximately 0.6 µ h^{-1}, but showed a complete recovery of growth over several hours (Fig. 7 C). At 50 µM concentration of hydrogen peroxide, the growth was severely affected. Initial growth rates of 0.2- 0.3 µ h^{-1} increased slowly over time but only partially recovered over the course of imaging (Fig. 7 D). When the hydrogen peroxide was increased to 100 µM, cellular growth was completely stalled during the entire duration of the imaging (Fig. 7 E). Overall, increasing concentrations of H_2O_2 resulted in a greater initial decrease in cell growth and increasingly impaired recovery of cell growth over time (Fig. 7 F).

Analysis of the average growth rate per microcolony over the duration of the experiment revealed that concentrations of H_2O_2 up to 30 µM had moderate effects on the average

408 growth rate, producing a decrease from 1.9 μ h^{-1} at 0 μM to 1.4 μ h^{-1} at 30 μM. Strong
409 reduction of growth was observed at exposure to 50 μM H_2O_2 with an average of 0.6 μ h^{-1},
410 and at 100 μM cell growth was negligible, with an average growth rate of 0.01 μ h^{-1} (Fig. 8 A).
411 The coefficients of variation for the average growth rates were low for the 0-30 μM H_2O_2
412 conditions, ranging from 0.09-0.24, while the variation for 50 μM H_2O_2 was extremely high at
413 0.75 (Fig. 8 B). For 100 μM H_2O_2 the coefficient of variation could not be accurately
414 calculated because the mean value of the growth rate was close to zero for most
415 microcolonies. Higher H_2O_2 concentrations were correlated with higher coefficient of
416 variation values (Fig. 8 C). Thus, an increase in H_2O_2 concentration was strongly correlated
417 with both a decrease in growth rate and an increase in growth rate variability, primarily for
418 the higher concentrations of stressor.

419 To analyze the relationship between Dps induction parameters and cellular growth, we
420 determined Pearson correlation coefficients between the average growth rate within
421 microcolonies and the intensity and the duration of induction peaks. Between the average
422 growth rate and amplitude of Dps induction for all stress conditions compared
423 simultaneously, we observed a strong negative correlation ($R = -0.71$) with a p value < 0.0001
424 (Fig. 5 B). Interestingly, the correlation coefficients calculated within each stress condition
425 were dramatically weaker, with an average of 0.03, and not significantly correlated.
426 Similarly, the correlation coefficient comparing the growth rate and the time to reach the
427 maximum fluorescence was strongly negative when calculated over all conditions ($R = -0.85$)
428 with a p value < 0.0001, but much weaker within each individual condition (average $R =$ -
429 0.18) (Fig. 5 C). Lower average growth rate was therefore seen to be strongly associated with
430 both higher Dps production and a longer induction time over a range of H_2O_2 concentrations.

We further analyzed the relationship between the mean fluorescence signal per colony and the mean growth rate per colony over time, identifying three response categories. The first category consisted of colonies that showed a constant high growth rate with a small-amplitude pulse or decrease over time of the fluorescence signal (Fig. 9A). In the second category, the colonies exhibited a steady increase of growth rate over time, starting around 0.5 $\mu\ h^{-1}$ and reaching values around 1.8-2 $\mu\ h^{-1}$. The fluorescence signal initially increased, reached its peak value, and then decreased again (Fig. 9B). The third category contained colonies in which the growth rate remained constantly low while the fluorescence signal increased robustly over time (Fig. 9C).

Increasing concentrations of H_2O_2 resulted in microcolony growth that was increasingly likely to exhibit a higher-numbered category of response, associated with increasingly impaired growth rate. All (100%) of the colonies grown without H_2O_2 showed Group I-type response (Fig. 9 D). Of the colonies grown in 10 µM H_2O_2, an intermediate behavior was seen in which 37% showed Group I response and 63% showed Group II response (Fig. 9 D). All (100%) of the colonies exposed to 30 µM H_2O_2 exhibited Group II response (Fig. 9 D). Of the colonies grown in 50 µM H_2O_2, an intermediate behavior was again seen in which 79% showed Group II behavior and 21% showed Group III response (Fig. 9 D). Finally, all (100%) of the colonies at 100 µM H_2O_2 showed Group III response (Fig. 9 D). The presence of these three distinct patterns may suggest a threshold model in which increasing stressor levels cause a recoverable reduction in growth rate at a lower threshold concentrations or a long-term halt in growth rate at a higher threshold concentration, due to still-uncharacterized internal regulatory processes.

Discussion

In this study we have investigated for the first time the Dps stress response at the single-cell level. When exposed to H_2O_2, *E. coli* cells exhibit a single pulse of activation of Dps production. Higher concentrations of H_2O_2 induce an increase in both the intensity and duration of the activation pulse. The correlation between cellular growth and stressor intensity is quite non-linear. Low H_2O_2 concentrations initiate a robust Dps response but have little effect on cellular growth, while higher concentrations of H_2O_2 slow down the growth rate dramatically and cause high variability. Cells exposed to the same H_2O_2 concentration do not receive a growth advantage in case of higher Dps induction. The recovery from stress may thus rely more upon the degree of damage generated in individual cells than to the strong induction of specific stress response proteins.

Stressor intensity predicts pulse amplitude and duration but not growth rate variability

The single pulse of induction of Dps production likely arises from more general features of the oxidative stress-induced response in *E. coli*. In the presence of H_2O_2, *dps* activation is regulated by the OxyR protein (25), a key regulator of the adaptive response to oxidative stress (47, 48). During exponential growth, H_2O_2 converts OxyR protein to an oxidized active form that recruits δ^{70}-RNA polymerase to initiate *dps* transcription (25). In *E. coli* cells treated with 200 µM H_2O_2, OxyR was fully converted to its oxidized form within 30 seconds of exposure to the stressor. Thereafter, OxyR reverted back to its reduced form with a half-life of ~ 5 minutes, and no oxidized OxyR was detected after 10 minutes (49). This transient activation response provides a potential window for *dps* transcription lasting only on the

477 order of minutes. Specific analysis of *dps* transcription kinetics in cells exposed to 10 µM
478 H_2O_2 revealed *dps* induction to be active for a limited period of time as well. Maximum levels
479 of *dps* transcript were detected at 1 minute after exposure, followed by a steady decrease
480 until returning to background levels by 20 minutes post exposure (50). Following the
481 decrease of OxyR activity, transcriptional repression of *dps* occurs via the formation of an
482 unproductive complex between the nucleoid-associated protein Fis and δ^{70} on the *dps*
483 promoter (26), that may provide stringent downregulation of *dps* transcription at the end of
484 its pulse of activation. The initial increase in observed Dps reporter signal intensity is thus
485 likely due to the transient burst of *dps* transcriptional activity. Thereafter, the decrease in
486 signal intensity likely derives from a combination of transcriptional repression of the *dps*
487 promoter and an increase in cellular growth rate that dilutes the reporter protein (Fig. 7),
488 with a minor contribution from photobleaching of the reporter protein (Fig. S5). The absence
489 of a decrease in signal intensity at the highest concentration of H_2O_2 (Fig. 2E,F) can be
490 explained by the near-zero cellular growth rate in this condition (Fig. 7E,F) that results in a
491 lack of dilution of the reporter protein.

492 We observe a correlation between the amount of stress applied to the cells and the peak
493 intensity of the Dps response, which saturates at the highest concentrations of stressor (Fig.
494 3). A correlation between the magnitude of the stress and the duration of the Dps response
495 is also indicated by our observations (Fig. 4), so that stronger stresses are associated with
496 both longer and stronger Dps production. The lack of increase in the peak intensity of the
497 Dps response between our highest two concentrations of H_2O_2 (Fig. 3A) seems to indicate a
498 saturation of the Dps production mechanism, perhaps due to the limited number of OxyR
499 regulatory molecules present in the cells. The speed of the initial increase of protein
500 production was seen to be similar under all conditions, such that stronger Dps responses are

501 achieved by modulation of the duration of production. However, not all bacterial stress
502 response genes show a similar pattern of expression. In *Bacillus subtilis*, the addition of
503 increasing concentrations of stressors results in production of the general stress response
504 factor σ^B with either an increase in peak amplitude but no alteration in the duration of the
505 response (35) or an increase in the frequency of pulses of induction, accompanied by only
506 weak changes in pulse amplitude and duration (33). In contrast, the highly modulated
507 duration of the Dps response under varying intensities of oxidative stress may be a strategy
508 to allow for an extended period of repair under conditions of more extensive damage.

509 Over a range of H_2O_2 concentrations, lower average growth rate is strongly correlated with
510 both stronger Dps production and a longer induction time (Fig. 5). Interestingly, cells
511 exposed to the same concentration of H_2O_2 do not receive a growth advantage from
512 increased levels of Dps production but instead exhibit similar or slower growth, even in the
513 50 μM H_2O_2 condition where Dps production levels varied by up to 4-fold. This observation
514 indicates that the kinetics of recovery from stress are not dictated by the magnitude of
515 induction of specific stress response enzymes. Rather, we propose that individual cells may
516 vary significantly in their amount of oxidative damage, such that cells sustaining more
517 damage both have slower growth and induce a larger stress response. The development of
518 real-time *in vivo* markers of oxidative damage will be quite interesting for study of the
519 relationship between damage and stress response induction.

520 Analysis of the stress conditions separately reveals that a low dose of H_2O_2 does not result in
521 a major reduction in cell growth rate, although the Dps enzyme is already produced (Fig. 1,
522 7). When the H_2O_2 concentration reaches a critical level, the bacteria exhibit extremely high
523 variability in growth rate. This variability does not correlate with either the intensity or the

variability of Dps production (Fig. 3, 8). Noise in metabolic gene expression has been shown to affect the growth stability of a cell under conditions of active metabolism (32). While metabolic reactions are crucial to synthesize enzymes and molecules necessary for cell development, stress response processes are responsible for maintaining the stability of cellular equilibrium under disruptive conditions. The observed variation in cell growth during exposure to high levels of oxidative stress might be linked to increased stochastic noise of one or more essential metabolic pathways under these conditions.

Cell-to-cell variability in Dps production is greater between microcolonies

The Dps response to oxidative stress shows some features of excitable dynamics, a class of transient cellular differentiation in which cells probabilistically enter into an ON state and return to the initial OFF state after a certain stereotypical period of time (51). Within the resolution of our experiments, we detect a single burst of protein production that rapidly activates a temporary stress-response state (Fig. 1, 2). Unlike a true excitable noise-triggered system, the return to an OFF state is not stereotypical in the case of Dps production. Instead, the return to the initial state occurs after a variable period of time that partially depends on growth kinetics. Additionally, we do not observe probabilistic entry into the ON state. Instead, every cell that was exposed to hydrogen peroxide was seen to initiate Dps production, and the kinetics and amplitude of the stress response were synchronized over each microcolony throughout the duration of imaging.

Cells lacking the *dps* gene are more sensitive to oxidative stress, showing dramatically reduced viability and elevated DNA damage (16, 18, 23). Because the Dps protein is a key

547 protector in stress survival, especially during the initial stage of the exposure, the non-
548 probabilistic initiation of Dps production allows all affected cells to respond to the oxidative
549 damage. The similar kinetics of the Dps response among individual cells within microcolonies
550 is likely a consequence of the majority of the active Dps production taking place in the
551 single-cell stage, before the founding cell has undergone cell division. Once an oxidatively
552 damaged cell resumes growth, the profile of the response is primarily reflective of dilution
553 only, which seems to exhibit low variation (Fig. 1).

554 The profile of the Dps response showed greater variability between different microcolonies
555 exposed to the same amount of stress than among different cells within microcolonies (Fig.
556 1, 2). While some of this variability may originate from non-homogeneous distribution of
557 hydrogen peroxide in the environment, a relatively moderate amount of site-to-site
558 variability was observed on the agarose pads. The variability between microcolonies was
559 seen to be dramatically higher for stressor concentrations in which the microcolonies were
560 seen to fall into either of two different patterns of growth and expression behavior rather
561 than only one (Fig. 2, 9). Most of the variability observed in the Dps responses is likely due to
562 differences between the progenitor cells of each individual colony. Non-genetic cell-to-cell
563 heterogeneity within a clonal population is common to many biological processes (34) and
564 can arise from a broad range of phenomena including noise in gene expression or
565 intracellular protein concentration, stochastic biochemical interactions, or non-synchronicity
566 in cell cycle stage (30, 52-54). A genome-wide survey of phenotypic noise over
567 approximately 75% of *E. coli* promoters found that stress-response genes such as *dps* exhibit
568 particularly variable expression during non-stressful growth (54). On top of this baseline
569 variability, we find that the variability in Dps production activity can increase more than
570 three-fold between non-stress and high-stress conditions (Fig. 2). Whether this dramatic

increase in variability under stress or upregulation is a common feature of all bacterial genes or is limited to certain functional classes will require further investigation.

Acknowledgements

We are grateful to Ilja Westerlaken, Mathia Arens, Sriram Tiruvadi Krishnan, Charl Moolman and Daniel Lam for fruitful discussions. We thank Prof. Nynke Dekker for her kind gift of the pROD22 plasmid and Prof. Christophe Danelon for the pRESET-mCherry strain.

The authors have no conflicts of interest.

Funding

This work was supported by the Netherlands Organization for Scientific Research (NWO/OCW), as part of the Frontiers of Nanoscience program under grant number NF13BNS10, and the Department of Bionanoscience of the Delft University of Technology.

References

1. **Ron E.** 2013. Bacterial Stress Response, p 589-603. *In* Rosenberg E, DeLong E, Lory S, Stackebrandt E, Thompson F (ed), The Prokaryotes doi:10.1007/978-3-642-30141-4_79. Springer Berlin Heidelberg.
2. **Gross CA, Chan C, Dombroski A, Gruber T, Sharp M, Tupy J, Young B.** 1998. The functional and regulatory roles of sigma factors in transcription. Cold Spring Harb Symp Quant Biol **63:**141-155.
3. **Paget MS, Helmann JD.** 2003. The sigma70 family of sigma factors. Genome Biol **4:**203.
4. **Gruber TM, Gross CA.** 2003. Multiple sigma subunits and the partitioning of bacterial transcription space. Annu Rev Microbiol **57:**441-466.
5. **Hengge-Aronis R.** 2002. Signal transduction and regulatory mechanisms involved in control of the sigma(S) (RpoS) subunit of RNA polymerase. Microbiol Mol Biol Rev **66:**373-395.
6. **Battesti A, Majdalani N, Gottesman S.** 2011. The RpoS-mediated general stress response in Escherichia coli. Annu Rev Microbiol **65:**189-213.
7. **Korshunov S, Imlay JA.** 2010. Two sources of endogenous hydrogen peroxide in Escherichia coli. Mol Microbiol **75:**1389-1401.
8. **Imlay JA.** 2013. The molecular mechanisms and physiological consequences of oxidative stress: lessons from a model bacterium. Nat Rev Microbiol **11:**443-454.
9. **Imlay JA.** 2008. Cellular defenses against superoxide and hydrogen peroxide. Annu Rev Biochem **77:**755-776.
10. **Robinson JM.** 2009. Phagocytic leukocytes and reactive oxygen species. Histochem Cell Biol **131:**465-469.
11. **Lamb C, Dixon RA.** 1997. The Oxidative Burst in Plant Disease Resistance. Annu Rev Plant Physiol Plant Mol Biol **48:**251-275.
12. **He X, Tian Y, Guo L, Lux R, Zusman DR, Shi W.** 2010. Oral-derived bacterial flora defends its domain by recognizing and killing intruders--a molecular analysis using Escherichia coli as a model intestinal bacterium. Microb Ecol **60:**655-664.
13. **Cohen GM, d'Arcy Doherty M.** 1987. Free radical mediated cell toxicity by redox cycling chemicals. Br J Cancer Suppl **8:**46-52.
14. **Almiron M, Link AJ, Furlong D, Kolter R.** 1992. A novel DNA-binding protein with regulatory and protective roles in starved Escherichia coli. Genes Dev **6:**2646-2654.
15. **Choi SH, Baumler DJ, Kaspar CW.** 2000. Contribution of dps to acid stress tolerance and oxidative stress tolerance in Escherichia coli O157:H7. Appl Environ Microbiol **66:**3911-3916.
16. **Nair S, Finkel SE.** 2004. Dps protects cells against multiple stresses during stationary phase. Journal of Bacteriology **186:**4192-4198.
17. **Jeong KC, Hung KF, Baumler DJ, Byrd JJ, Kaspar CW.** 2008. Acid stress damage of DNA is prevented by Dps binding in Escherichia coli O157: H7. Bmc Microbiology **8**.
18. **Martinez A, Kolter R.** 1997. Protection of DNA during oxidative stress by the nonspecific DNA-binding protein Dps. J Bacteriol **179:**5188-5194.
19. **Meyer AS, Grainger DC.** 2013. The Escherichia coli Nucleoid in Stationary Phase. Adv Appl Microbiol **83:**69-86.
20. **Zhao GH, Ceci P, Ilari A, Giangiacomo L, Laue TM, Chiancone E, Chasteen ND.** 2002. Iron and hydrogen peroxide detoxification properties of DNA-binding protein from starved cells - A ferritin-like DNA-binding protein of Escherichia coli. Journal of Biological Chemistry **277:**27689-27696.
21. **Grant RA, Filman DJ, Finkel SE, Kolter R, Hogle JM.** 1998. The crystal structure of Dps, a ferritin homolog that binds and protects DNA. Nature Structural Biology **5:**294-303.

22. **Bozzi M, Mignogna G, Stefanini S, Barra D, Longhi C, Valenti P, Chiancone E.** 1997. A novel non-heme iron-binding ferritin related to the DNA-binding proteins of the Dps family in Listeria innocua. J Biol Chem **272:**3259-3265.
23. **Karas VO, Westerlaken I, Meyer AS.** 2015. The DNA-Binding Protein from Starved Cells (Dps) Utilizes Dual Functions To Defend Cells against Multiple Stresses. J Bacteriol **197:**3206-3215.
24. **Azam TA, Iwata A, Nishimura A, Ueda S, Ishihama A.** 1999. Growth phase-dependent variation in protein composition of the Escherichia coli nucleoid. Journal of Bacteriology **181:**6361-6370.
25. **Altuvia S, Almiron M, Huisman G, Kolter R, Storz G.** 1994. The dps promoter is activated by OxyR during growth and by IHF and sigma S in stationary phase. Mol Microbiol **13:**265-272.
26. **Grainger DC, Goldberg MD, Lee DJ, Busby SJ.** 2008. Selective repression by Fis and H-NS at the Escherichia coli dps promoter. Mol Microbiol **68:**1366-1377.
27. **Yamamoto K, Ishihama A, Busby SJ, Grainger DC.** 2011. The Escherichia coli K-12 MntR miniregulon includes dps, which encodes the major stationary-phase DNA-binding protein. J Bacteriol **193:**1477-1480.
28. **Ali Azam T, Iwata A, Nishimura A, Ueda S, Ishihama A.** 1999. Growth phase-dependent variation in protein composition of the Escherichia coli nucleoid. J Bacteriol **181:**6361-6370.
29. **Brehm-Stecher BF, Johnson EA.** 2004. Single-cell microbiology: tools, technologies, and applications. Microbiol Mol Biol Rev **68:**538-559, table of contents.
30. **Elowitz MB, Levine AJ, Siggia ED, Swain PS.** 2002. Stochastic gene expression in a single cell. Science **297:**1183-1186.
31. **Junker JP, van Oudenaarden A.** 2014. Every cell is special: genome-wide studies add a new dimension to single-cell biology. Cell **157:**8-11.
32. **Kiviet DJ, Nghe P, Walker N, Boulineau S, Sunderlikova V, Tans SJ.** 2014. Stochasticity of metabolism and growth at the single-cell level. Nature **514:**376-379.
33. **Locke JC, Young JW, Fontes M, Hernandez Jimenez MJ, Elowitz MB.** 2011. Stochastic pulse regulation in bacterial stress response. Science **334:**366-369.
34. **Martins BM, Locke JC.** 2015. Microbial individuality: how single-cell heterogeneity enables population level strategies. Curr Opin Microbiol **24:**104-112.
35. **Young JW, Locke JC, Elowitz MB.** 2013. Rate of environmental change determines stress response specificity. Proc Natl Acad Sci U S A **110:**4140-4145.
36. **Gibson DG, Young L, Chuang RY, Venter JC, Hutchison CA, Smith HO.** 2009. Enzymatic assembly of DNA molecules up to several hundred kilobases. Nature Methods **6:**343-U341.
37. **Guzman LM, Belin D, Carson MJ, Beckwith J.** 1995. Tight regulation, modulation, and high-level expression by vectors containing the arabinose PBAD promoter. J Bacteriol **177:**4121-4130.
38. **Reyes-Lamothe R, Possoz C, Danilova O, Sherratt DJ.** 2008. Independent positioning and action of Escherichia coli replisomes in live cells. Cell **133:**90-102.
39. **Young JW, Locke JC, Altinok A, Rosenfeld N, Bacarian T, Swain PS, Mjolsness E, Elowitz MB.** 2012. Measuring single-cell gene expression dynamics in bacteria using fluorescence time-lapse microscopy. Nat Protoc **7:**80-88.
40. **Schneider CA, Rasband WS, Eliceiri KW.** 2012. NIH Image to ImageJ: 25 years of image analysis. Nat Methods **9:**671-675.
41. **Csoka B, Nagy G.** 2004. Determination of diffusion coefficient in gel and in aqueous solutions using scanning electrochemical microscopy. Journal of Biochemical and Biophysical Methods **61:**57-67.
42. **Gendron PO, Avaltroni F, Wilkinson KJ.** 2008. Diffusion Coefficients of Several Rhodamine Derivatives as Determined by Pulsed Field Gradient-Nuclear Magnetic Resonance and Fluorescence Correlation Spectroscopy. Journal of Fluorescence **18:**1093-1101.
43. **Boulineau S, Tostevin F, Kiviet DJ, ten Wolde PR, Nghe P, Tans SJ.** 2013. Single-cell dynamics reveals sustained growth during diauxic shifts. PLoS One **8:**e61686.

44. **Carroll P, James J.** 2009. Assaying Promoter Activity Using LacZ and GFP as Reporters, p 265-277. *In* Parish T, Brown AC (ed), Mycobacteria Protocols, vol 465. Humana Press.
45. **Otsuka Y, Muto A, Takeuchi R, Okada C, Ishikawa M, Nakamura K, Yamamoto N, Dose H, Nakahigashi K, Tanishima S, Suharnan S, Nomura W, Nakayashiki T, Aref WG, Bochner BR, Conway T, Gribskov M, Kihara D, Rudd KE, Tohsato Y, Wanner BL, Mori H.** 2015. GenoBase: comprehensive resource database of Escherichia coli K-12. Nucleic Acids Res **43:**D606-617.
46. **Nghe P, Boulineau S, Gude S, Recouvreux P, van Zon JS, Tans SJ.** 2013. Microfabricated polyacrylamide devices for the controlled culture of growing cells and developing organisms. PLoS One **8:**e75537.
47. **Christman MF, Storz G, Ames BN.** 1989. OxyR, a positive regulator of hydrogen peroxide-inducible genes in Escherichia coli and Salmonella typhimurium, is homologous to a family of bacterial regulatory proteins. Proc Natl Acad Sci U S A **86:**3484-3488.
48. **Tao K, Makino K, Yonei S, Nakata A, Shinagawa H.** 1991. Purification and characterization of the Escherichia coli OxyR protein, the positive regulator for a hydrogen peroxide-inducible regulon. J Biochem **109:**262-266.
49. **Aslund F, Zheng M, Beckwith J, Storz G.** 1999. Regulation of the OxyR transcription factor by hydrogen peroxide and the cellular thiol-disulfide status. Proc Natl Acad Sci U S A **96:**6161-6165.
50. **Michan C, Manchado M, Dorado G, Pueyo C.** 1999. In vivo transcription of the Escherichia coli oxyR regulon as a function of growth phase and in response to oxidative stress. J Bacteriol **181:**2759-2764.
51. **Eldar A, Elowitz MB.** 2010. Functional roles for noise in genetic circuits. Nature **467:**167-173.
52. **Davey HM, Kell DB.** 1996. Flow cytometry and cell sorting of heterogeneous microbial populations: the importance of single-cell analyses. Microbiol Rev **60:**641-696.
53. **Schwabe A, Bruggeman FJ.** 2014. Contributions of cell growth and biochemical reactions to nongenetic variability of cells. Biophys J **107:**301-313.
54. **Silander OK, Nikolic N, Zaslaver A, Bren A, Kikoin I, Alon U, Ackermann M.** 2012. A genome-wide analysis of promoter-mediated phenotypic noise in Escherichia coli. PLoS Genet **8:**e1002443.

Figure legends

Fig. 1. Exposure to H_2O_2 induces a single pulse of Dps production activity synchronized over the individual cells within each microcolony. A-E) Examples of fluorescence intensity over time in individual cells in a microcolony exposed to different concentrations of H_2O_2. Each line represents a single cell. F) The average coefficient of variation (CV) over time of the fluorescence intensity among all the cells exposed to the same stress condition, for varying concentrations of H_2O_2.

Fig. 2. The Dps response per microcolony exhibits variation in peak amplitude and duration. A-E) The average fluorescence signal over time of microcolonies exposed to different concentrations of H_2O_2. Each line represents the average fluorescence intensity of all cells within one microcolony. F) The average fluorescence signal over time of all the colonies exposed to the same stress condition. The shaded area represents the standard deviation. G) The coefficient of variation (CV) over time of the average fluorescence signals of all the microcolonies exposed to the same stress condition, for varying concentrations of H_2O_2.

Fig. 3. Dps induction intensity increases with exposure to higher concentrations of H_2O_2. A) The average maximum values of the fluorescence signal for each microcolony, for each concentration of H_2O_2. The error bars represent the standard deviation. The letters represent the statistical significance: samples labeled with different letters are statistically different (ANOVA test, $p < 0.05$). B) The maximum values of the fluorescence signal for each microcolony, and the coefficient of variation (CV) of the maximum fluorescence intensity among microcolonies, for each H_2O_2 concentration. C) Scatter plot of the coefficient of

variation vs. the average maximum fluorescence value for each concentration of H_2O_2. R represents the Pearson correlation coefficient.

Fig. 4. The duration of Dps induction increases with exposure to higher concentrations of H_2O_2. A) The average time at which the maximum value of the fluorescence signal was observed for each microcolony, for each concentration of H_2O_2. The error bars represent the standard deviation. The letters represent the statistical significance: samples labeled with different letters are statistically different (ANOVA test, $p < 0.05$). B) The time to the maximum value of the fluorescence signal for each microcolony, and the coefficient of variation (CV) of the time to the maximum fluorescence intensity among microcolonies, for each H_2O_2 concentration. C) Scatter plot of the coefficient of variation vs. the time to the average maximum fluorescence value for each concentration of H_2O_2. R represents the Pearson correlation coefficient.

Fig. 5. Correlations between growth rate, intensity, and duration of Dps induction. A) Scatter plot of the average maximum fluorescence intensity vs. the average time to the maximum fluorescence for individual microcolonies. B) Scatter plot of the average growth rate per colony vs. the average maximum fluorescence intensity for individual microcolonies. C) Scatter plot of the average growth rate per colony vs. the average time to the maximum fluorescence intensity for individual microcolonies. Each dot represents a single microcolony. Microcolonies exposed to the same H_2O_2 concentration are represented in the same color. The R value in the top right corner of each graph represents the Pearson correlation coefficient over all the data. The R below the label for each concentration of H_2O_2 represents the R value calculated over all microcolonies in each stress condition. * = $p<0.05$.

Fig. 6. Effects of oxidative stress on cellular length. A) Distribution of the length of all cells in a microcolony, averaged over all timepoints within each experiment, for different concentrations of H_2O_2. The top and bottom of the vertical bars represent the maximum and the minimum length values, respectively; the top and bottom of the rectangular box represent the 75^{th} and the 25^{th} percentile; the horizontal line within the box is the median; and the square in the box is the mean value. The letters represent the statistical significance: samples with different letters are statistically different (ANOVA test, $p < 0.05$). B) The average length of all cells within the microcolonies over time, for varying concentrations of H_2O_2. The shaded areas represent the standard deviation.

Fig. 7. Oxidative stress suppresses initial rates of cellular growth. A-E) The average instantaneous growth rate of all the cells within a colony over time, for different concentrations of H_2O_2. Each line represents the average growth rate of all cells within one microcolony. F) The average growth rate over time of all the colonies in the presence of the same concentration of H_2O_2. The shaded areas represent the standard deviation.

Fig. 8. Variation in microcolony growth rate increases at lower growth rates. A) The average growth rate per microcolony, averaged over all cells over all timepoints for each microcolony, for each concentration of H_2O_2. The error bars represent the standard deviation. The letters represent the statistical significance: samples labeled with different letters are statistically different (ANOVA test, $p < 0.05$). B) The average growth rate for each microcolony, and the coefficient of variation (CV) of growth rate among microcolonies, for each H_2O_2 concentration. Two of the microcolonies exposed to 50 μM H_2O_2 and ten of the microcolonies exposed to 100 μM H_2O_2 are not visible in the plot because their average

792 growth rate is 0. C) Scatter plot of the coefficient of variation vs. the average growth rate for
793 each concentration of H_2O_2. R represents the correlation coefficient. *= $p < 0.05$.
794
795 **Fig. 9.** Microcolonies exhibited three categories of Dps response. A-C) Scatter plots of the
796 mean fluorescence signal and the mean growth rate per microcolony, over time, for example
797 microcolonies in each category. Each dot represents the average fluorescence and the
798 average growth rate of a single microcolony at a specific timepoint, colored to indicate the
799 timepoint. A) Category I: a constant high growth rate associated with a slightly decreasing,
800 low fluorescence signal. B) Category II: a steady increase in growth rate over time associated
801 with a pulse of fluorescence signal. C) Category III: a robust increase in fluorescence signal
802 over time associated with a constant low growth rate. D) The percentage of microcolonies in
803 each response category, for each concentration of H_2O_2. The letters represent the statistical
804 significance: samples in each group labeled with different letters are statistically different
805 (two-sample *t*-test; $p < 0.05$).

Fig. 1

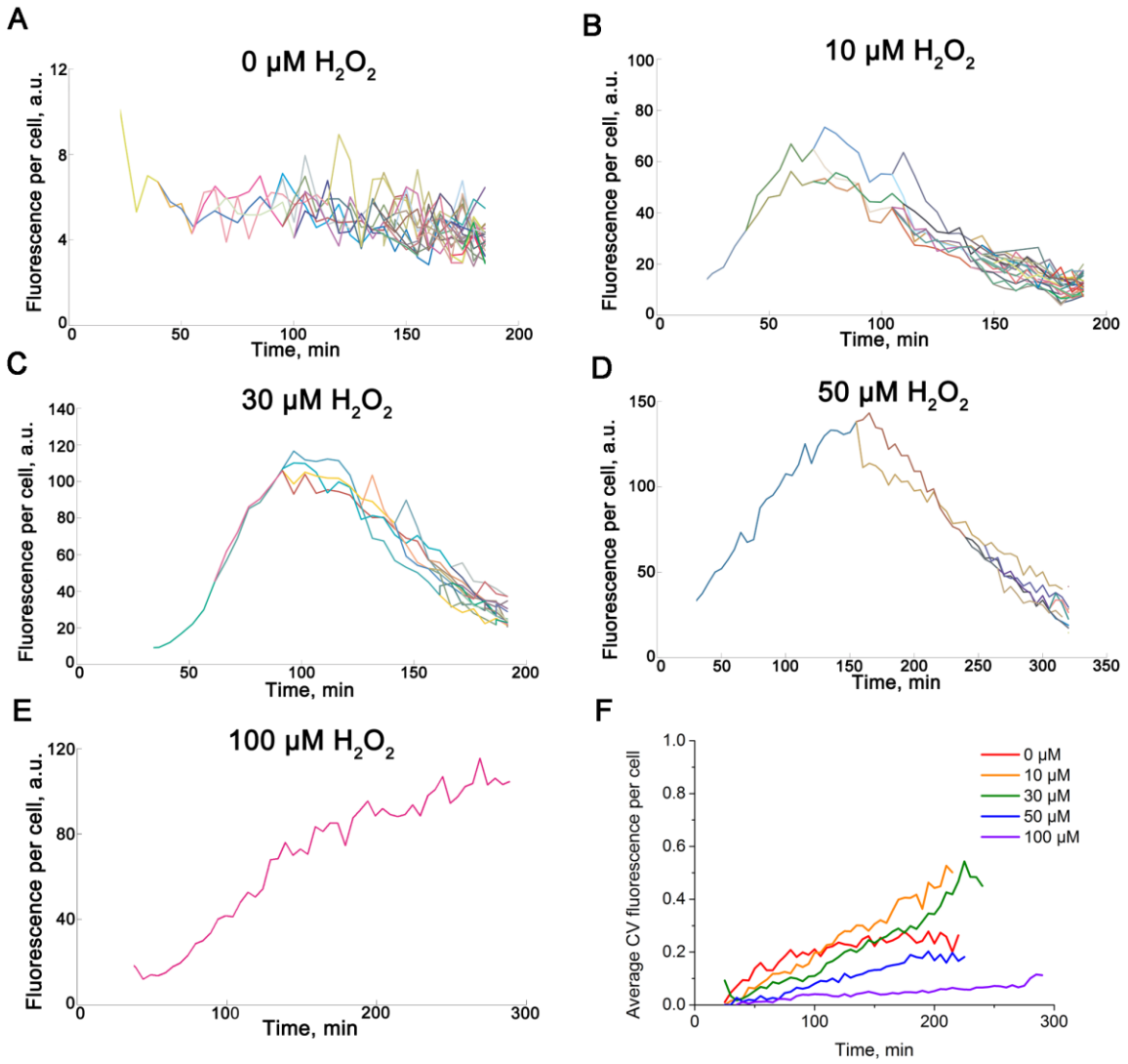

Fig. 1. Exposure to H_2O_2 induces a single pulse of Dps production activity synchronized over the individual cells within each microcolony. A-E) Examples of fluorescence intensity over time in individual cells in a microcolony exposed to different concentrations of H_2O_2. Each line represents a single cell. F) The average coefficient of variation (CV) over time of the fluorescence intensity among all the cells exposed to the same stress condition, for varying concentrations of H_2O_2.

Fig. 2

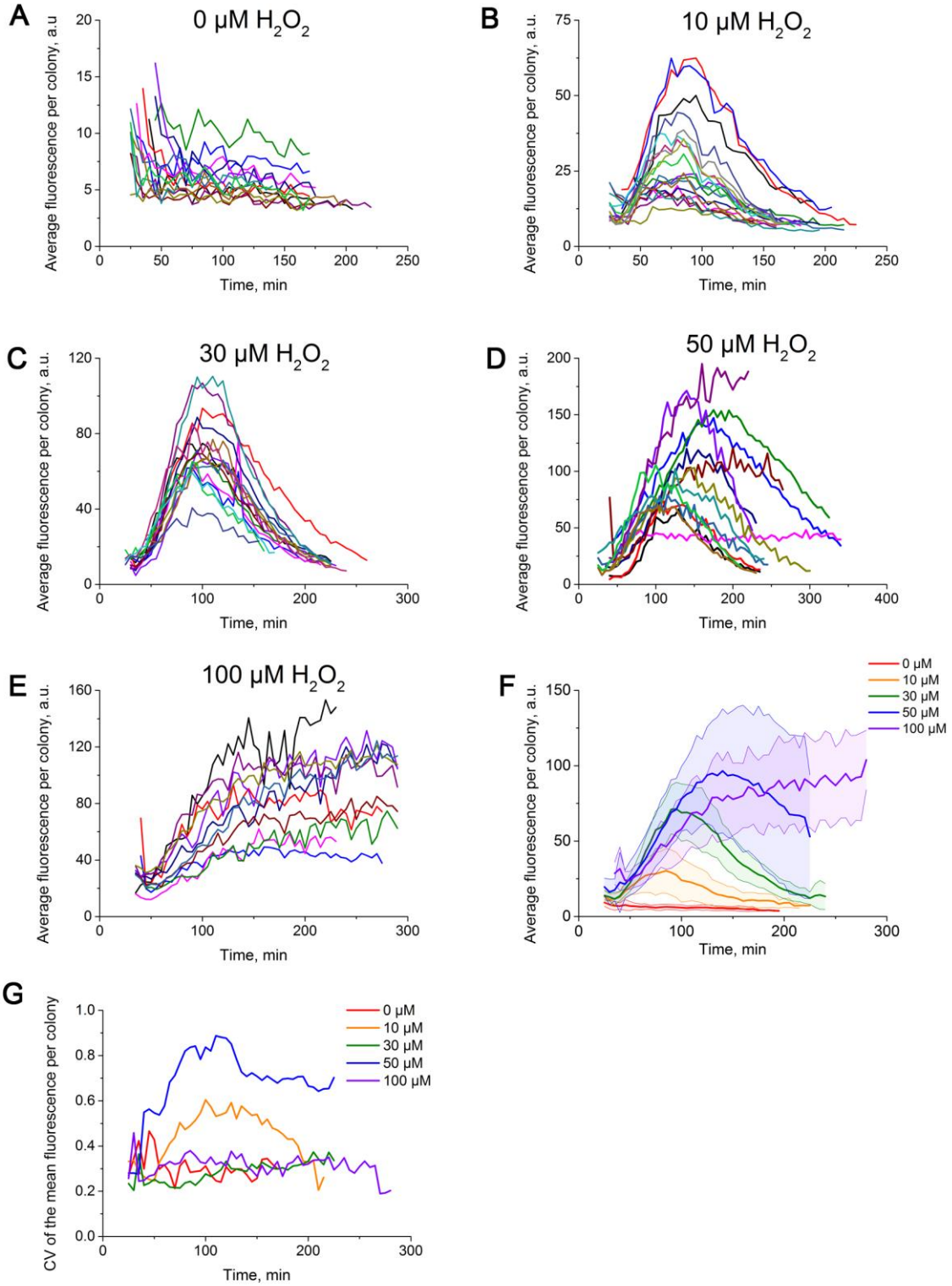

Fig. 2. The Dps response per microcolony exhibits variation in peak amplitude and duration. A-E) The average fluorescence signal over time of microcolonies exposed to different

concentrations of H_2O_2. Each line represents the average fluorescence intensity of all cells within one microcolony. F) The average fluorescence signal over time of all the colonies exposed to the same stress condition. The shaded area represents the standard deviation. G) The coefficient of variation (CV) over time of the average fluorescence signals of all the microcolonies exposed to the same stress condition, for varying concentrations of H_2O_2.

Fig. 3

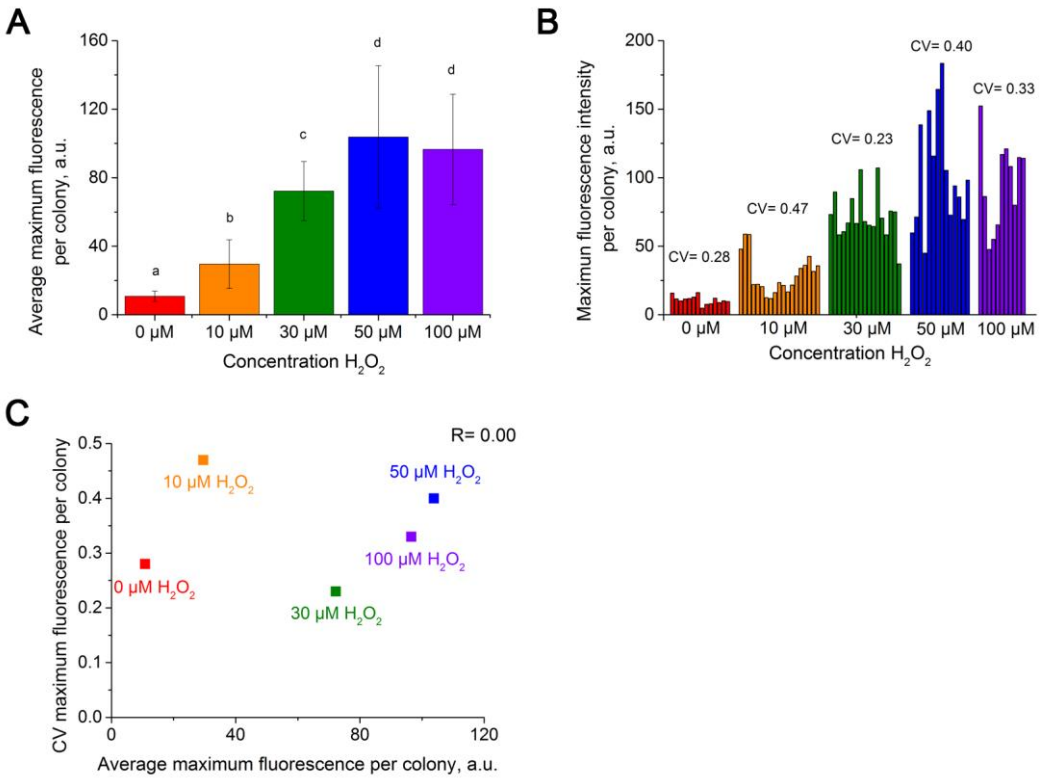

Fig. 3. Dps induction intensity increases with exposure to higher concentrations of H_2O_2. A) The average maximum values of the fluorescence signal for each microcolony, for each concentration of H_2O_2. The error bars represent the standard deviation. The letters represent the statistical significance: samples labeled with different letters are statistically different (ANOVA test, $p < 0.05$). B) The maximum values of the fluorescence signal for each microcolony, and the coefficient of variation (CV) of the maximum fluorescence intensity among microcolonies, for each H_2O_2 concentration. C) Scatter plot of the coefficient of variation vs. the average maximum fluorescence value for each concentration of H_2O_2. R represents the Pearson correlation coefficient.

Fig. 4

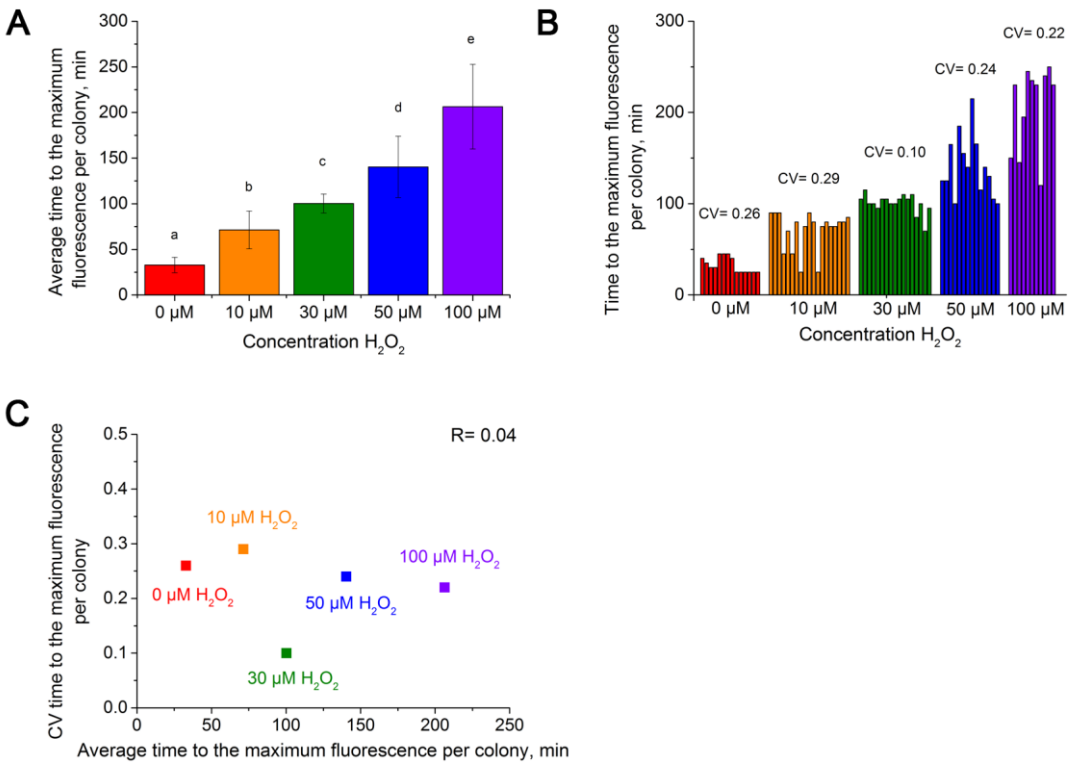

Fig. 4. The duration of Dps induction increases with exposure to higher concentrations of H_2O_2. A) The average time at which the maximum value of the fluorescence signal was observed for each microcolony, for each concentration of H_2O_2. The error bars represent the standard deviation. The letters represent the statistical significance: samples labeled with different letters are statistically different (ANOVA test, $p < 0.05$). B) The time to the maximum value of the fluorescence signal for each microcolony, and the coefficient of variation (CV) of the time to the maximum fluorescence intensity among microcolonies, for each H_2O_2 concentration. C) Scatter plot of the coefficient of variation vs. the time to the average maximum fluorescence value for each concentration of H_2O_2. R represents the Pearson correlation coefficient.

Fig. 5

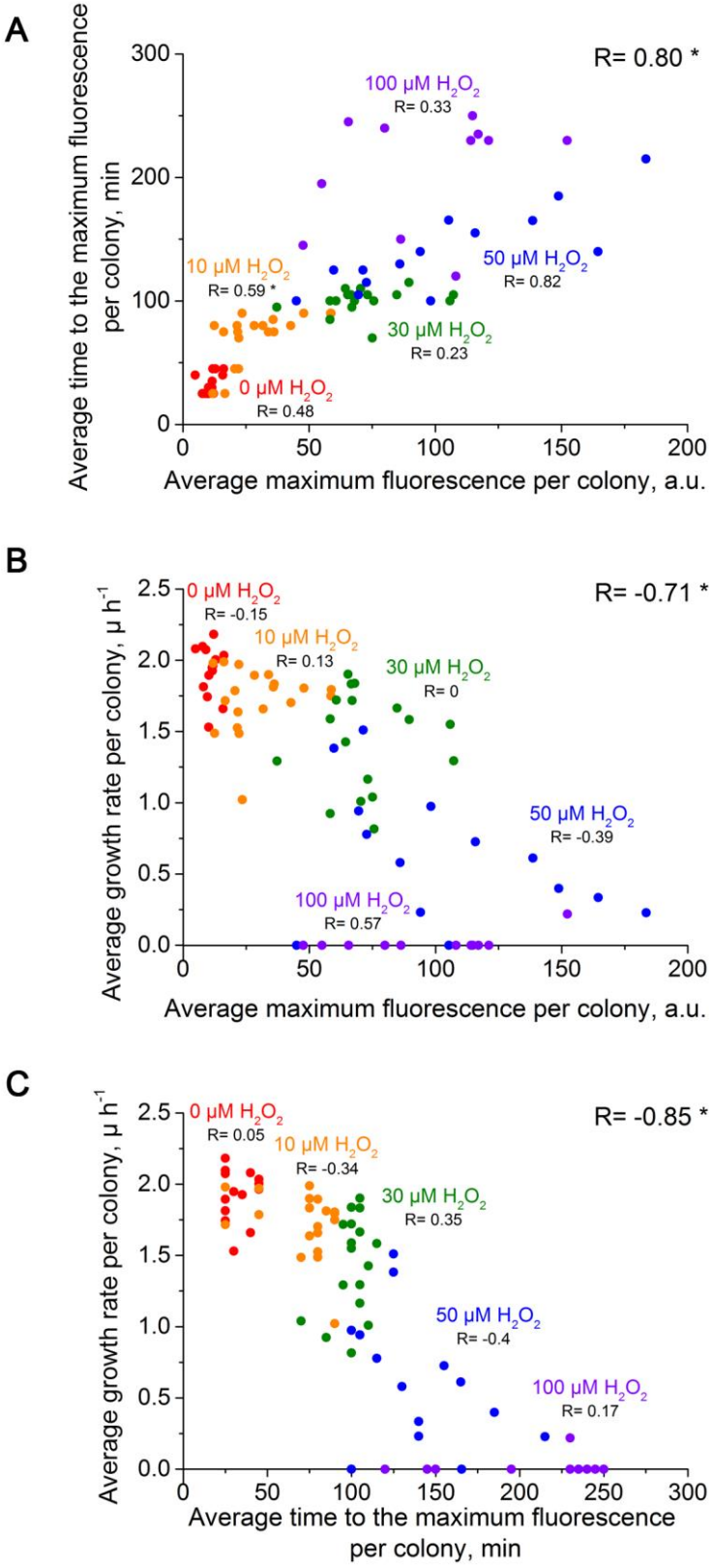

Fig. 5. Correlations between growth rate, intensity, and duration of Dps induction. A) Scatter plot of the average maximum fluorescence intensity vs. the average time to the maximum

fluorescence for individual microcolonies. B) Scatter plot of the average growth rate per colony vs. the average maximum fluorescence intensity for individual microcolonies. C) Scatter plot of the average growth rate per colony vs. the average time to the maximum fluorescence intensity for individual microcolonies. Each dot represents a single microcolony. Microcolonies exposed to the same H_2O_2 concentration are represented in the same color. The R value in the top right corner of each graph represents the Pearson correlation coefficient over all the data. The R below the label for each concentration of H_2O_2 represents the R value calculated over all microcolonies in each stress condition. * = $p<0.05$.

Fig. 6

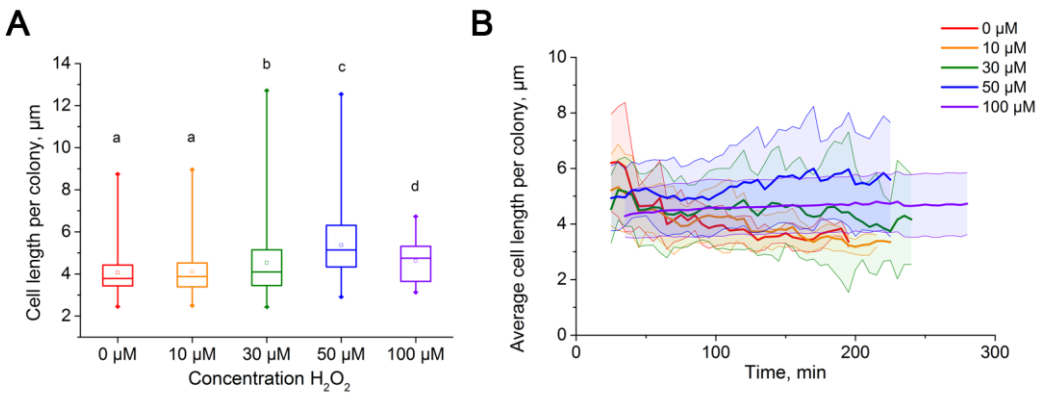

Fig. 6. Effects of oxidative stress on cellular length. A) Distribution of the length of all cells in a microcolony, averaged over all timepoints within each experiment, for different concentrations of H_2O_2. The top and bottom of the vertical bars represent the maximum and the minimum length values, respectively; the top and bottom of the rectangular box represent the 75^{th} and the 25^{th} percentile; the horizontal line within the box is the median; and the square in the box is the mean value. The letters represent the statistical significance: samples with different letters are statistically different (ANOVA test, $p<0.05$). B) The average length of all cells within the microcolonies over time, for varying concentrations of H_2O_2. The shaded areas represent the standard deviation.

Fig. 7

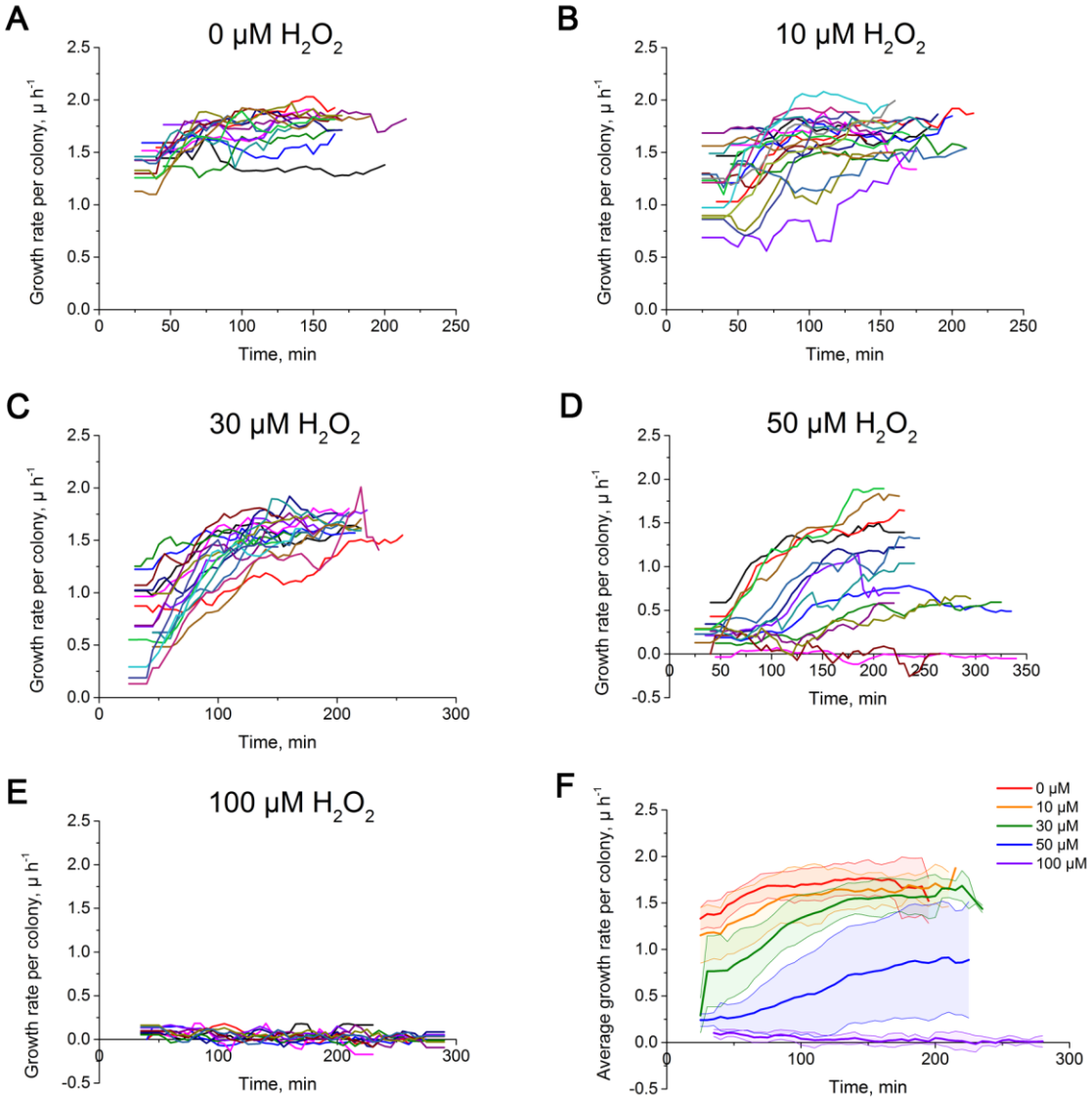

Fig. 7. Oxidative stress suppresses initial rates of cellular growth. A-E) The average instantaneous growth rate of all the cells within a colony over time, for different concentrations of H_2O_2. Each line represents the average growth rate of all cells within one microcolony. F) The average growth rate over time of all the colonies in the presence of the same concentration of H_2O_2. The shaded areas represent the standard deviation.

Fig. 8

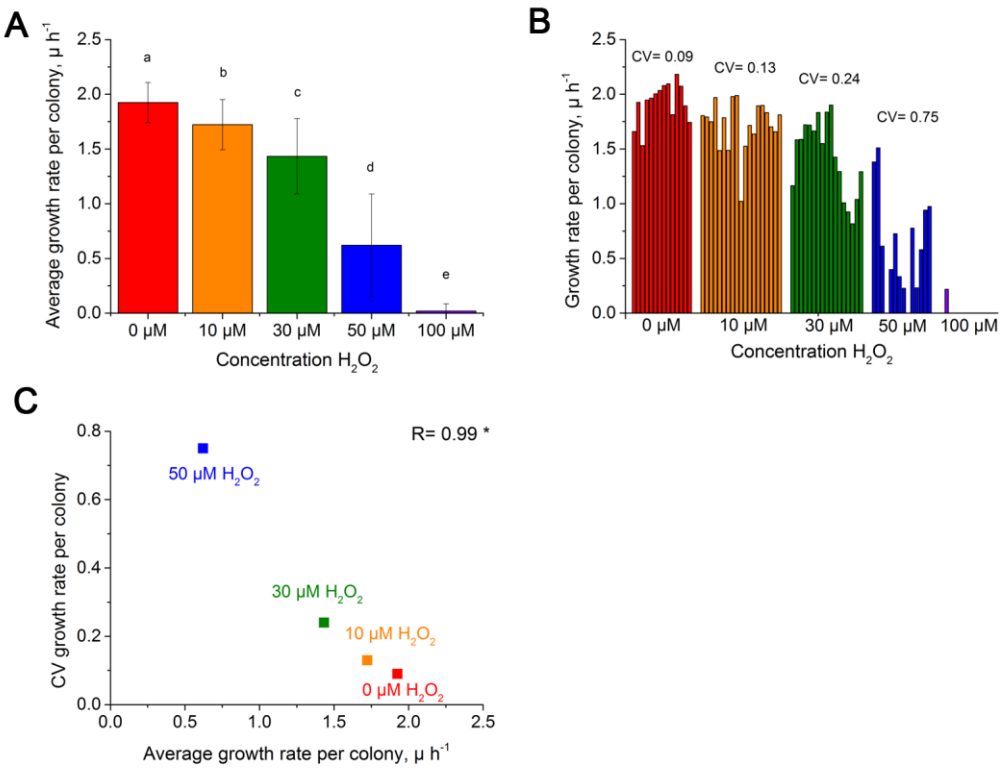

Fig. 8. Variation in microcolony growth rate increases at lower growth rates. A) The average growth rate per microcolony, averaged over all cells over all timepoints for each microcolony, for each concentration of H_2O_2. The error bars represent the standard deviation. The letters represent the statistical significance: samples labeled with different letters are statistically different (ANOVA test, $p < 0.05$). B) The average growth rate for each microcolony, and the coefficient of variation (CV) of growth rate among microcolonies, for each H_2O_2 concentration. Two of the microcolonies exposed to 50 µM H_2O_2 and ten of the microcolonies exposed to 100 µM H_2O_2 are not visible in the plot because their average growth rate is 0. C) Scatter plot of the coefficient of variation vs. the average growth rate for each concentration of H_2O_2. R represents the correlation coefficient. *= $p < 0.05$.

Fig. 9

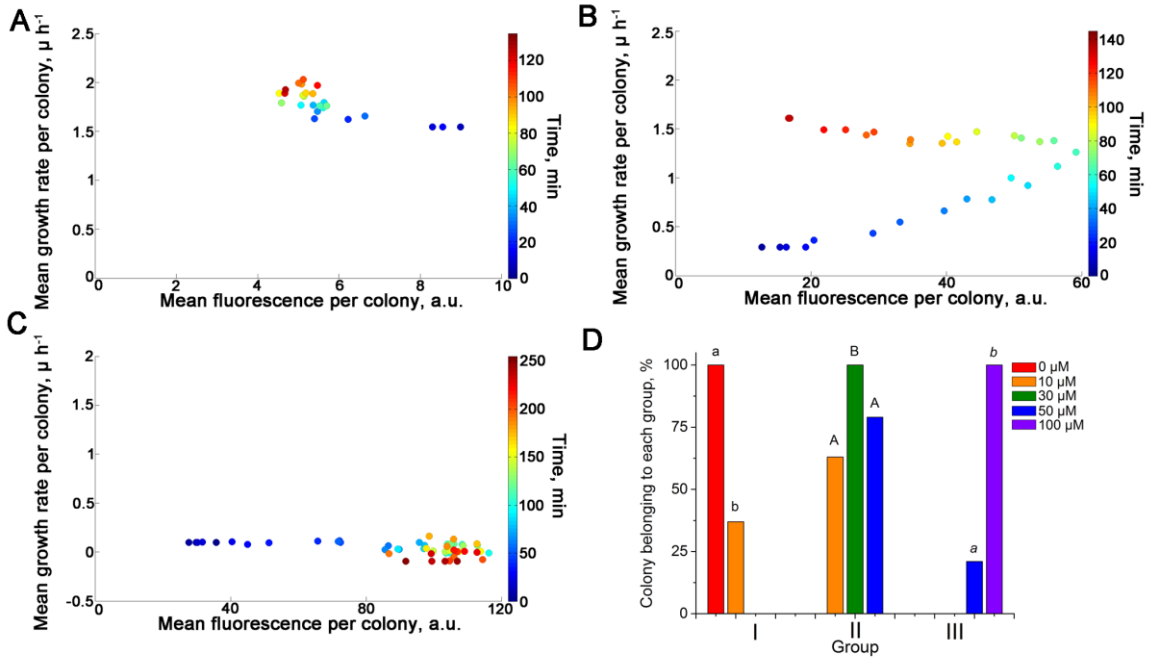

Fig. 9. Microcolonies exhibited three categories of Dps response. A-C) Scatter plots of the mean fluorescence signal and the mean growth rate per microcolony, over time, for example microcolonies in each category. Each dot represents the average fluorescence and the average growth rate of a single microcolony at a specific timepoint, colored to indicate the timepoint. A) Category I: a constant high growth rate associated with a low fluorescence signal. B) Category II: a steady increase in growth rate over time associated with a pulse of fluorescence signal. C) Category III: a robust increase in fluorescence signal over time associated with a constant low growth rate. D) The percentage of microcolonies in each response category, for each concentration of H_2O_2. The letters represent the statistical significance: samples in each group labeled with different letters are statistically different (two-sample *t*-test, $p < 0.05$).